Ultra-Hydrophilic Transition Metals as Histophilic Biomaterials

Herbert P. Jennissen

Institut für Physiologische Chemie; Universität Essen, Hufelandstr. 55,
D-45122 Essen, Germany
E-mail: hp.jennissen@uni-essen,de

Summary: Extremely hydrophilic surfaces have been prepared on titanium, stainless steel and cobalt chromium alloys after treatment by a chromosulfuric acid method at 200-240 °C. In spite of a ca. 300-500-fold higher surface roughness (Ra ~ 880-1100 nm) in comparison to the quartz glass controls (Ra ~ 2 -3 nm), surfaces with contact angles close to 0° in the absence of contact angle hysteresis (ultra-hydrophilic surfaces) were obtained. We have called this phenomenon "Inverse Lotus Effect". Metal surface layers exhibiting such properties form excellent priming coats with bioadhesive properties (histophilic surfaces) for the attachment of biocoats consisting of BMP-2 with bioactive properties in bone. Direct immobilization of BMP-2 on implant surfaces eliminates the need for a separate BMP-2 carrier or delivery system such as collagen, as is widely employed by others. A fundamental problem in such surfaces is that it is not at all certain that a protein immobilized in such a manner will retain its biological activity. In the case of BMP-2 it can be shown in vitro that the novel surfaces are biologically active. Similarly in vivo studies indicate an accelerated and improved osseointegration

Keywords: biomaterials; surfaces; ultra-hydrophilic transition metals

Introduction

Biomaterials and implantology as a whole have had a major impact on medical therapy in the last 50 years. There have also been setbacks as experienced several years ago with breast implants [1]. What is often overlooked is the fact that the most successful implants in medicine are of metallic origin and in this group are headed by titanium. Implant lifetimes in patients with titanium alloy hip implants in the range of 10-15 years are no rarity and are unsurpassed by any other biomaterial such as polymers. Therefore it is of highest interest to understand metallic biocompatibility. In addition research on metal surfaces such as titanium should be increased with the aim of further improving longevity and compatibility of titanium based implants.

Several years ago we discovered a novel wet chemical etching method with chromosulfuric acid (CSA) at 200-240 °C for the preparation of extremely hydrophilic

 DOI: 10.1002/masy.200550705

surfaces on transition metals like titanium, steel (316L) [2], aluminum [3] and cobalt chromium (CoCrMo) alloys [4]. In subsequent work it was demonstrated that these metals with surface roughness values of Ra ~ 1 µm exhibited *ultra-hydrophilic* properties i.e. dynamic contact angles < 10° with absent contact angle hysteresis [5,6]. Only in the case of a TiO_2 polycrystalline anatase film, formed on a glass substrate and then irradiated by UV light had a similarly low but transient static contact angle been described up to that time [7]. Thus with a chemical and not physical method we have been able to produce such ultra-hydrophilic surfaces directly on transition metals [4-6] which are then stable for many weeks e.g. in methanol [8] or other solutions. We have employed ultra-hydrophilic CSA surfaces as a priming coat for the subsequent functionalization of the surface with biomolecules e.g. BMP-2 (= biocoat) [2,5,8-10]. Although the exact mechanism involved in the chromosulfuric acid-metal reaction leading to ultra-hydrophilic surfaces is unknown the phenomenon warrants a detailed treatment and discussion, which will be given in this paper.

Materials and Methods

Metal mini plates. Small electropolished titanium mini plates (cp titanium, grade 2; 15 x 10 x 0.8-1.0 mm; roughness factor r ~ 1.2-1.3), CoCrMo (CoCr29Mo). ISO 5832-4) and AISI 316L medicinal stainless steel (X2CrNiMo 18 15 3; DIN 17443; 1.4441) mini plates of the same size were employed with electropolished surfaces as described previously [2,5]. In addition titanium alloy miniplates (Ti-6Al-4V; Fa. GB Implantattechnologie, Essen, Germany) were coated on both sides by titanium plasma spray (TPS) [5,9] technology (plasma vapor deposition of cp titanium powder according to ISO 5832-2; DOT GmbH, Rostock, Germany) in a thickness of ~ 200 µm. These surfaces have an arithmetic average roughness of Ra ~ 30-35 µm, a maximal profile height (DIN) Ry ~ 180-200 µm (Prof. Dr. A. Fischer, Werkstofftechnik II, Universität Duisburg-Essen) and a roughness factor of r ~ 20 (Dipl.-Ing. C. Hessing, Institut für Werkstoffe, Bochum). Before use the mini plates were first treated in hot 5% HNO_3 as described [2]. Then they were "surface enhanced" by treatment with chromosulfuric acid (92% H_2SO_4, 1.3% CrO_3, density 1.84 g/cm³) under stirring at 230-240 °C for 60 minutes (= CSA-Ti plates, CSA-steel plates), washed and stored as described [2].

Quartz glass. Polished quartz glass (fused silica) slides (Suprasil I, Fa. Heraeus, Hanau) 10 x 25 x 1 mm were employed after polishing to a final surface roughness of 1-2 nm. These slides were repolished in the optical workshop of the University of Essen to a planarity of $\lambda/10$ and a final surface roughness of 1-2 nm (interference microscopy, Micromap 1.2 Interference Microscope, Ges. für Angew. Techn. & Opt. Systeme mbH, ATOS, Pfungstadt). The quartz glass slides were cleaned in chromosulfuric acid (Merck, Darmstadt; 92% H_2SO_4, 1.3% CrO_3, density 1.84 g/cm³) by heating to 90 °C for 60 minutes. The slides were taken out of the acid extensively washed with double distilled water, which had additionally been end-purified in a Milli-Q system (Millipore), followed by boiling in this pure water for 30 minutes. After extensive washing in this water the quartz glass slides were dried in a stream of nitrogen (quality 5) and immediately used for dynamic contact angle measurements in the Wilhelmy-Plate apparatus [2].

Dynamic contact angle measurements were performed in a constant temperature room (22 °C) according to the Wilhelmy Plate method with an immersion and emersion speed of 1 mm/min as described [2]. Before the measurements metal mini plates were cleaned with acetone (defatted) and air dried. After HNO_3 or chromosulfuric acid treatment the microplates were first washed in water and then boiled 30 minutes in 2% EDTA pH 7.0 and H_2O to be stored in dry methanol as described [2]. Before measuring the contact angles the alcohol was removed by evaporation. The uncertainty in the measurements is in the range of 1-2° (see also [11]). For all other methods including the chemical modification of the enhanced metal surfaces for coupling proteins, electrophoresis and animal experiments see ref. [2,5].

Surface functionalization with silane [12]. The HNO_3 or CSA treated air dried mini plates were reacted with 3-aminopropyl triethoxy silane (APS) in a Teflon holder in 47.5 ml toluene to which 2.5 ml APS had been added under inert gas. The system was then closed and heated to boiling under reflux for 3.5 hours under stirring. The mini plates were then washed 3 times in 10 ml trichloromethane, acetone and methanol and air dried (= APS mini plates or APS-CSA mini plates, ca. 1-2 nmol/cm^2).

Covalent coupling of rhBMP-2 [12]. For covalent protein coupling the Ti-APS- mini plates type II were activated by 1,1'-carbonyl diimidazole (CDI, 2.5 g/50 ml) in dry acetone under inert gas at room temperature for 4 hours under tumbling (Ti-CSA-APS-CDI mini plates). The CDI-activated plates were then washed in acetone, then in water and added to the protein solution. For immobilization of rhBMP-2 on the CDI-mini plates ^{125}I-CT-rhBMP-2 (ca. 0.1-

0.25 mg/ml) in 125 mM sodium borate, 0.066 % SDS, pH 10.0 (= borate buffer) for 12-14 hours at room temperature. The plates were washed 4 times with 2 ml borate buffer and immediately used for the bioassay.

Non-covalent immobilization (adsorption) of rhBMP-2 [4]. ^{125}I-CT-rhBMP-2 (ca. 10 µCi/mg) was adsorbed to titanium mini plates type II functionalized with 3-aminopropyl triethoxy silane (see above) by incubation for 12-14 hours in 0.1-0.25 mg/ml ^{125}I-CT-rhBMP-2 in borate buffer at room temperature as described previously. The plates were washed 4 times with 2 ml borate buffer and immediately used for the bioassay.

BMP-2. Recombinant human bone morphogenetic protein 2 (rhBMP-2) was prepared and radioactively labeled as described [5,12]. For in vitro cell culture experiments and in vivo experiments rhBMP-2 was prepared and immobilized under sterile conditions [5]. The biological activity of rhBMP-2 was determined with p-nitrophenol in microtiter wells as previously described [13]. The half-activation constants ($K_{0.5}$) of rhBMP-2 for the induction of alkaline phosphatase in MC3T3-E1 cells were in the range of 20-75 nM [4,13]. Radioactively labeled rhBMP-2 was prepared by the chloramine-T method (^{125}I-CT-rhBMP-2) as described [4].

Cell culture. Mouse calvaria osteoblast MC3T3-E1 cells (passages 4-12) were cultivated and grown as previously described [8].

In vitro biological activity measurement of immobilized rhBMP-2. The bioassay of immobilized BMP-2 activity (MC3T3-cell ALP-induction test) is based on the induction of alkaline phosphatase (ALP) in MC3T3-E1 cells by sterile BMP-2-titanium surface. $5x10^5$ fresh trypsinized cells were seeded on titanium mini plates as described [8]. After 6-12 hours the medium of the now confluent cells was replaced by α-MEM containing 1 % FCS and the cells were grown on the bioactive surface for 6 days [8]. After 6 d the cells were carefully rinsed three times with Dulbecco's phosphate buffer and fixed with 2 % paraformaldehyde for 10 min and permeabilized by washing with DPBS/Tween 20 0.2 % (v/v) [8]. Activity of alkaline phosphatase was visualized with the endogenous phosphatase detection kit ELF-97 (Molecular Probes, Inc., Oregon, USA) under a fluorescence microscope as previously described [8].

Theoretical Considerations

Wettability and contact angles

The wettability of a solid surface is generally characterized by the pure water contact angle (θ) of a sessile drop at ambient temperature [11,14-22]. Thermodynamically the contact angle at the equilibrium of the interfacial tensions (σ) is described by the Young equation [14]:

$$\sigma_{sv} = \sigma_{sl} + \sigma_{lv} \cos \theta_o \qquad (1)$$

where σ_{sv} , σ_{sl} and σ_{lv} are the interface tensions of the contacting phase boundaries of the liquid (l), the solid (s) and the vapor phase (v), with θo the equilibrium contact angle. On a

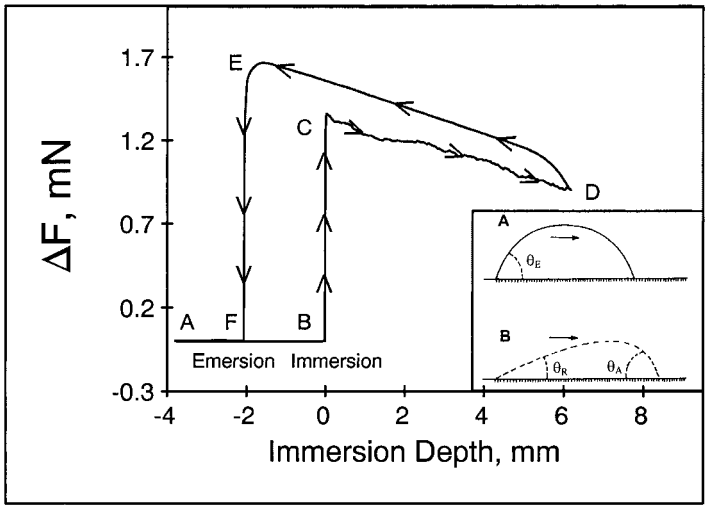

Fig. 1: Immersion-force trajectories obtained in a Wilhelmy Plate apparatus for the determination of dynamic contact angles.
Trajectory A-B-C-D: immersion; trajectory D-E-F-A: emersion
A-B: Weight force of plate
B-C: = ΔF_A = Advancing contact angle (θ_A) dependent force increase
C-D: Buoyancy dependent decrease in force due to immersion
D-E: Buoyancy dependent increase in force due to emersion
E-F: = ΔF_R = Receding contact angle (θ_R) dependent force decrease
(This value is normalized to 0 mm immersion.)
Insert: A. Movement of a drop of water on an ideal surface with equilibrium contact angle (θ_E):
B. Movement of a drop of water on a real surface, advancing contact angle (θ_A), receding contact angle (θ_R). See ref. [17].

The dynamic contact angel is calculated according to: $\cos \theta = \frac{\Delta F}{\rho \cdot \gamma_2}$
ΔF = force difference, ρ = density of liquid

theoretical basis a surface is wettable at a $\theta_0 < 90°$, and not wettable at $\theta_0 > 90°$. It is completely wetted at $\theta_0 = 0$ and completely non-wettable at $\theta_0 = 180°$. On a practical basis the beginning of a reasonable wetting is generally defined as beginning at contact angles below 60° [19]. The Young equation is strictly valid only for ideal surfaces, which are perfectly smooth, homogenous and placed horizontal to gravity. Quasi-ideal surfaces of this type are generally only found on single crystals or freshly split mica.

One of the most powerful procedures for measuring contact angles is the dynamic method [6,15,17]. If an initially sessile drop of water is moved at equilibrium on an ideal homogeneous and perfectly smooth surface horizontal to gravity, it can be moved back and forth without any deformation or change in the contact angle θ_0 (**Fig. 1, insert A**). In the case of a real, inhomogeneous surface however, movement induces a deformation of the drop (**Fig. 1, insert B**) with the generation of two different contact angles on the advancing (θ_A) and the receding side (θ_R) of the drop respectively (see [6]). Since the advancing contact angle is less sensitive to inhomogeneities on the surface than the receding angle it is considered the decisive angle [16] corresponding most closely to the sessile drop angle ($\theta_0 \approx \theta_A$). Dynamic contact angles can be determined with high precision by the method of Wilhelmy (see [15] and **Fig. 1**).

Contact angle hysteresis

As seen above, if one moves a drop of pure water on an ideal smooth surface under equilibrium conditions one obtains only a single contact angle (**Fig. 1, insert A**). On real surfaces especially because of the surface inhomogeneity moving the drop deforms it and leads to two different contact angles (**Fig. 1, insert B**). The larger the difference between these angles the more the differential force trajectories will separate and as a rule the more non-ideal the surface will be. This phenomenon is called contact angle hysteresis.

Contact angle hysteresis is defined quantitatively as the difference between the advancing θ_A and the receding θ_R contact angle:

$$H = \Delta\theta = \theta_A - \theta_R \qquad (2)$$

The liquid/gas interface which moves as the contact line of the measurement over the surface (advancing trajectory) does not return along the advancing trajectory but along the receding trajectory to the point of origin. As a result of the different trajectories two different contact angles result. The spreading of a drop of water is thus a thermodynamically irreversible process linked to a dissipation of energy. Thermodynamic irreversibility is due to local energy barriers and metastable states of microscopic and nanoscopic domains on the surface (see [23]).

Contact angle hysteresis is generally caused by surface inhomogeneities, which may be of chemical or structural nature. Chemical inhomogeneities might originate from oxidation, corrosion, coatings, grain boundaries or crystallographic anisotropies. Structural inhomogeneities originate mainly from surface roughness properties. In the past a surface roughness of > 100 nm [15] was thought to elicit contact angle hysteresis. Today there is evidence that already a surface roughness of > 10 nm will cause contact angel hysteresis [16].

Rough surfaces can be subdivided into two classes [24] those based on (i) classical surfaces with only three interfaces as defined by the Young equation (eq. 1) and those based on (ii) composite interfaces which e.g. contain entrapped air. Composite surfaces are often found for $\theta > 90°$ and apply to the ultra-hydrophobic surfaces (see also ref. [25])of the plant kingdom displaying the "Lotus Effect" [26] (see below).

The influence of surface roughness on the equilibrium (static) contact angle was first described by the Wenzel in his famous equation [21,22]:

$$\cos \theta_{AS} = r \cos \theta_{GS} \tag{3}$$

where θ_{AS} corresponds to the static contact angle of the actual surface (i.e. rough or total surface), θ_{GS} to the static contact angle of the geometric surface (i.e. ideal smooth surface). The constant r is the roughness factor ($r = \cos \theta_{AS}/\cos \theta_{GS}$), which can also be defined as the surface area ratio [21]:

$$r = \frac{actual\ surface}{geometric\ surface} \tag{3a}$$

For the case that $\theta_{GS} < 90°$ then $\theta_{AS} < \theta_{GS}$ and for $\theta_{GS} > 90°$ then $\theta_{AS} > \theta_{GS}$. Thus on a hydrophilic surface an increase in roughness factor will lead to a reduction of the contact

angle whereas on a hydrophobic surface the same increase in surface roughness will lead to an enhancement of the contact angle. In a more exact definition the roughness factor is defined by Johnson and Dettre [24] as:

$$r = \frac{\Omega^{SL}}{A} \qquad (4)$$

Where Ω^{SL} corresponds to the solid-liquid interfacial area and A to the plane area under the drop. Hugh and Mason [27] have modified the Wenzel equation by introducing a surface texture factor ϕ. There have also been other treatments of contact angle hysteresis by Cassie [28,29] considering a "patchwork" arrangement of homogenous elements or Marmur [30] who introduced the intrinsic contact angle. A generalized Young equation based on Cassie's and Wenzel's laws has also been proposed [31]. Since in all of these cases additional information on surface domains, textures etc. are necessary the discussion here will be limited to the Wenzel [21] and Johnson and Dettre [24,32] approaches.

Surface roughness

Surface roughness is considered the main cause of contact angle hysteresis [16,18], since it leads to an increase in surface area (see eq. 3). It will therefore be treated briefly. A surface profile can be subdivided into a low frequency (waviness) and high frequency (roughness) component. The high frequency surface profile in a defined length-interval or trace-length (e.g. 5.6 mm) corresponds to the surface roughness. Usually the trace length is broken down further into a cut-off length (e.g. 0.8 mm). For calculations a reference line for the profile is set such that the area of the hills and valleys is equal. A typical measure of the surface roughness is the Ra value which corresponds to the "arithmetic average roughness" or the absolute deviation of the profile above and below the profile reference line (see [6,33]) for which the following equation is valid:

$$Ra = \frac{1}{L}\int z \cdot dx \qquad (5)$$

z is the absolute distance from the reference line to a positive or negative profile height on the y-axis. L is defined as the trace length along the x-axis. The sum of the absolute values of the positive and negative profile heights is called the maximal profile height Ry. If profile height measurements are made at equally spaced intervals along the trace, a simplified equation can be use for calculating the Ra value (see [6]):

$$R_a = (z_1 + z_2 + z_3 + \ldots z_n)/n \qquad (6)$$

Besides the arithmetic average roughness (Ra) a "root mean square" or geometric average roughness (Rq) may also be calculated [33], which will not be discussed here. Finally it should be noted that surfaces with identical Ra-Values do not necessarily have the same surface profiles.

Hydrophilicity and Hydrophobicity

Hydrophilicity and hydrophobicity are terms which apply to and are restricted to aqueous systems. In non-aqueous systems the surface properties are often described as lipophilicity or oleophilicty [7]. Since life evolved in water the discussion will be restricted to aqueous systems.

Hydrophilicity of a glass surface can be defined as the spreading tendency of water on such a surface leading to a wetting due to non-covalent attractions (e.g. van-der Waals, hydrogen bonding) between the two phases (i.e. adhesion). Hydrophilicity generally implies a high surface energy. Although the spreading of a sessile drop begins when the diameter of the drop contact ("footprint") exceeds the diameter of the spherical drop itself (i.e. at $\theta_A < 90°$) the beginning of a reasonable wetting is generally defined as beginning at contact angles below 60° [19].

The hydrophobicity of a surface is correlated to the decreased spreading tendency of water (water repulsion) on such a surface leading to a rounded drop resulting from a loss of non-covalent interactions (i.e. adhesion). Hydrophobicity generally implies a low surface energy. The loss of water adhesion properties on a hydrophobic surface does not however mean that a chemically non-interacting surface is created. Although a so-called low energy surface is formed hydrophobic surfaces in aqueous media exhibit a new type of attraction

towards molecules other than water (e.g. proteins) based on hydrophobic interactions (see [34]). Non-covalent interactions of the hydrophobic type have been described as "the unusually strong attraction between non-polar molecules and surfaces in water" [35]. The hydrophobic attraction energy for two interacting methane molecules is ca. 6-fold higher in water than the van der Waals interaction energy in vacuum and has been estimated to ca. -8.5 kJ mol^{-1} [35,36]. Hydrophobic interactions are based on the extrusion of a monomolecular layer of ordered water molecules covering two adjacent hydrophobic surfaces into less-ordered bulk water with a concomitant increase in entropy. Under the condition of $\Delta H << T\,\Delta S$ the Gibbs free Energy is negative ($-\Delta G \approx T\,\Delta S$) constituting an entropy driven reaction (see review [37]).

However the above terms are not at all as clear as they might seem [38]. Clean glass and a hydrogel like poly(2-hydroxyethyl methacrylate) both give contact angles close to zero and are therefore termed hydrophilic by that criterion. However the interfacial free energy in the case of the glass/water interface is large, whereas in the case of the poly(2-hydroxyethyl methacrylate)/water interface it is close to zero [38]. This might also explain some paradox properties of hydrogels [37]. Hydrogels should therefore be treated differently than solid surfaces and the simple equating of lubricity with hydrophilicity in the case of hydrogels [19] may require rethinking and the introduction of additional parameters. A solution to these problems has been suggested by the breaking down of the surface tension into a dispersive (non-polar) and polar components respectively [39].

The model of critical surface tensions according to Baier [40]

In respect to a histophilic ("tissue loving") or osteophilic ("bone loving") behavior of implants the phenomenon of wettability plays a decisive role. A histophilic surface shows an enhanced capacity for tissue interactions. The term "osteophilic" can be traced to work by Thomas [41] and today is not limited to a specific surface. In general it implies an osteoconducting surface. In contrast bioactive surfaces [2,5] actively lead to a de novo bone formation on the implant surface.

Originally Baier [40] suggested in a model in 1972 a correlation between biocompatibility, bioadhesion and the critical surface tension of solids (γ_C). This is summarized in **Table 1**, in which additionally the respective contact angles have been calculated [11,22] . In the model of Baier, that was originally developed for the blood-biomaterial contact, the "zone of good biocompatibility" lies in the hydrophobic range at 20-

32 dyn/cm (θ = 114° – 145°) and die "zone of bioadhesion" lies in the hydrophilic range at 42-72 dyn/cm (θ = 0 - 90°). The "zone of strong bioadhesion" lies in the range of 68-72 dyn/cm (θ = 0 - 31°). Until now it has not been possible to prove that biocompatibility correlates with a range of 20-32 dyn/cm. This failure as a biocompatibility parameter is also

Table 1: Scaling of Critical Surface Tensions, Wettability and Relative Biological Reactivity (Modified According to the Model of Baier (1972).

Critical surface tension (γ_C) dynes/cm	Calculated Advancing Contact Angle (θ_{SLV})	Wettability with Water	Relative Biological Interaction	Biological Zone
	180°	Ultra-hydrophobic		
20	145°		weak	Hypothetical Zone of Biocompatibility
32	114°	Hydrophobic		
40	96°		Medium	Zone of good Bioadhesion
50	77°	Hydrophilic		
60	55°		Strong	
70	22°			
71.5	10°	Ultra-hydrophilic		
72	0°			

The basic equation underlying the calculation of critical surface tensions was proposed by Zisman [22] (for review see [11]): $\cos \theta_{SLV} = 1 - \beta (\gamma_L - \gamma_C)$ where θ_{SLV} is the advancing surface-liquid-vapor contact angle, β is a constant of the value ~0.035 [11], γ_L is the surface tension of the liquid (for H_20 at 25 °C γ_L is 72 dyne/cm) and γ_C is the critical surface tension. This equation allows the approximate calculation of the contact angle for a critical surface tension if γ_L is known. This is illustrated in Table 1 together with the model of Baier [40]. For further details see Theoretical Considerations, the text and ref. [5,6].

due to the fact that in 1972 the decisive role of hydrophobic interactions in protein adsorption was not generally known, and it had been wrongly concluded that proteins are not adsorbed on low energy surfaces. In the past there have been several futile attempts define zones of good biocompatibility for biomaterials, so that up to today there are no general criteria for defining biocompatibility. On the other hand there is little controversy concerning the hypothesis of a "zone of good bioadhesion" (see **Table 1**) in the hydrophilic range i.e. at high critical surface tensions and small contact angles. The strongly interacting zone between 0-10° could thus be called the *histophilic* zone. Here it has been shown in several papers [42,43], that cell adhesion and cell spreading display a sigmoidal dependence on the surface energy (γs). In the hydrophobic range at $\gamma s < \sim 60$ dyn/cm practically no adhesion of fibroblasts can

be observed. On the other hand at surface energies $\gamma s > \sim 60$ dyn/cm a significant to strong adhesion and spreading of cells has been reported. The dependence of adhesion for certain strains of bacteria [44] appears quite different in that the adhesion curves run through a maximum at contact angles between 70-90°. In contrast to fibroblasts the bacteria did not adhere between 0-50°. A major problem in these studies is however that the adhesion dependence was not measured on one substratum type modified to display different contact angles but on a large number of different polymers and glass. Thus it cannot be excluded that in some cases specific polymer effects determine adhesion and not the wettability i.e. contact angle.

Similarly on hydrophilic titanium surfaces an enhanced spreading and adhesion of blood and bone-marrow cells has also been reported. [45,46]. However current titanium implant surfaces as employed clinically for endosseous implants must in general be regarded as hydrophobic [12,47]. On the other hand the strongest bioadhesion is to be expected in the ultra-hydrophilic range (**Table 1**). Therefore extensive work has been undertaken in this direction [2,5,6].

In conclusion the model of Baier has had an important heuristic impact in the area of biomaterials research and even today it is often employed as a guiding principle. How could one understand the model of Baier on a molecular level? Mechanistically one has to go back to the first reaction between a biomaterial and the organism, which is protein adsorption. At high contact angles i.e. in the hydrophobic range different proteins are adsorbed than in the hydrophilic range at low contact angles. The adsorbed protein layers consisting of different proteins on the surface could therefore result in differential tissue reactions [6], which in the hydrophilic range would lead to a stronger bioadhesion. In addition it should be considered that the adsorbed protein layer itself leads to a change in the contact angle and the surface energy [6].

The Lotus Effect

The occurrence of non-wettable surfaces in the plant kingdom has been known for many decades in botany as well as in physical chemistry [48]. Several years ago attention was again attracted to these extremely hydrophobic surfaces on the grounds that these surfaces are not smooth but rough and microstructured (see **Fig. 2**) [26]. On the leaves of the lotus flower and

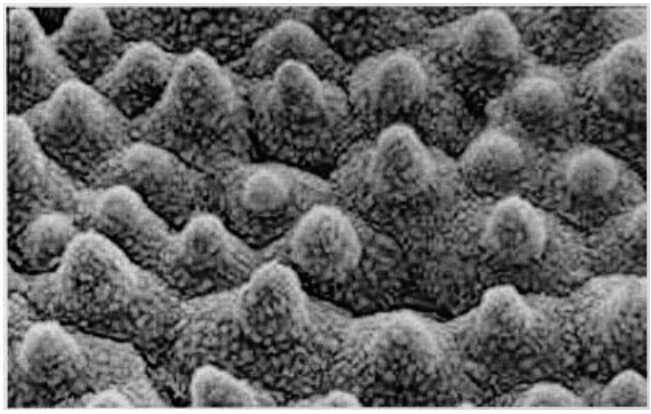

Fig. 2: Scanning electron micrograph of the rough adaxial double structured leaf surface of a plant (Nelumbo nucifera) exhibiting the "Lotus-Effect" .
The microstructure (diameter of epidermal papillae ca. 50 µm) consists mainly of epicuticular wax cristalloids. A nano-like finer structure (0.2-5 µm) can be detected on the papillae and the mound-like structures underneath. (By permission of Prof. W. Barthlott, see ref. [26]).

other plants contact angles of 160° are measured, which endow the leaves with self-cleaning properties (see **Fig. 3**). Due to the high contact angles (hydrophobicity) and the microstructure of the cuticle drops of water which adsorb surface contaminants freely roll off the non-adhesive surface keeping the leaf surface clean ("Lotus-Effect"). The Lotus Effect begins at

Fig. 3: Rolling drop of water on a slanted Lotus leaf displaying the self-cleansing properties of the Lotus-Effect.
Contaminating dust particles adhere to the surface of the water drop and are removed from the leaf as the drop rolls off leaving a clean track behind. (By Permission of Prof. W. Barthlott, see ref. [26]).

contact angles of ca. 130° and is fully developed at 160° (see **Table 2**) [26]. Lotus Effect displaying interfaces are there fore microscopically rough, extremely hydrophobic surfaces, displaying a self-cleansing effect. The special wetting characteristics (contact angles > 160°) are due to the high roughness of a composite surface containing air enclosures in a special array of micro structures. This is in agreement with the finding of nano-bubbles on very hydrophobic artificial surfaces (see ref. [25]). In short one could call the Lotus Effect an apparent hydrophobic effect through surface roughness. The effect so defined appears in full agreement with the Wenzel equation (eq. 3), that on a hydrophobic surface ($\theta_{GS} > 90°$) an increase in surface roughness (i.e. surface area) will lead to larger contact angles. However micro- and nano-bubbles also play a decisive role. Plants appear to have optimized the above law. The self-cleansing effect is an extra gift of the ultra-hydrophobic system.

Table 2: Static Contact Angles of Plant leaves.

Plant	Contact Angle, °
Brassica oleracea	160.3 ± 0.8
Colocasia esculenta	159.7 ± 1.4
Mutisia decurrens	128.4 ± 3.6
Nelumbo nucifera (Lotus)	160.4 ± 0.7

Mean values (±SD) of 20 measurements of the static contact angle (°) on the adaxial leaf surfaces of the species used for contamination experiments. (From Barthlott and Neinhuis [26] by permission)

Ultra-Hydrophilic Metal Surfaces

The titanium surface

The biocompatibility of titanium is intimately related to the oxide layer on its surface. This oxide layer has been shown to consist in the majority of cases of titanium dioxide (TiO_2,

Ti(IV)). What is often not realized is the omnipresence of TiO_2 in our environment, being contained in skin creams and cosmetics (sunscreens [49]) and coming into contact with our outer body surface. It also occurs in our foods (whitener [50]) and many oral pharmaceuticals [51,52] thus having contact with our inner body surface. Finally TiO_2 is often used as a white tattoo pigment [53] being injected sub/intracutaneously and of course is most widespread on the surface of bone endoprostheses coming into contact with bone marrow, bone tissue, muscle and connective tissue. After ^{44}Ti injection (i.p.) in the rat ^{44}Ti can be detected in all tissues and it is excreted both in urine and feces [54]. In spite of the above extensive usage allergic reactions to TiO_2 are extremely rare to absent [55]. Thus TiO_2 is probably the most biocompatible material known at present.

Titanium dioxide comes in four different modifications: non-crystalline and the distinct crystal forms anatase, rutile and cotunnite [56]. Commercially available titanium metal (c.p.

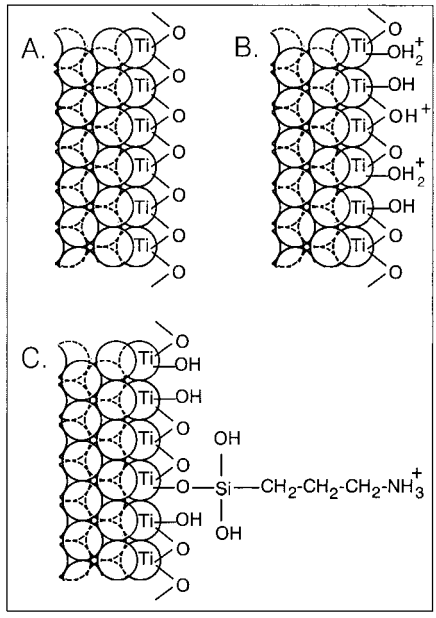

Fig. 4: Schematic model of titanium with titanium dioxide surface layer and silanized layer.

A. Non-hydrolyzed oxide Layer. B. hydrolyzed oxide Layer with protonated groups at pH below the isoelectric point. At neutral pH a negative surface results due to deprotonation of bridging hydroxyls. C. Functionalization of TiO_2 surface layer with aminopropyl triethoxy silane leading to a covalent oxane bond between a terminal hydroxyl and the silane reagent. At neutral pH a positive surface results. For further details see text and ref. [57]

titanium) is generally coated by rutile [58] a six-coordinate complex, which is more stable than anatase. The non-hydrolyzed, non-protonated oxide layer is shown schematically in **Fig. 4A**. Pure titanium dioxide surfaces contain two types of hydroxyl groups (see **Fig. 4B**) in equal proportions situated either on bridging or terminal oxygen atoms [57]. For such surfaces points of zero charge at pH 5.8 [57] and isoelectric points at pH 4.5 [59,60] have been reported. The chemical reaction for terminal hydroxyls may be represented as consisting of a protonation reaction forming the cationic species $\equiv TiOH_2^+$ and a deprotonation reaction forming the anionic species $\equiv TiO^-$:

$$\equiv TiOH_2^+ - H^+ \leftrightarrows \equiv TiOH - H^+ \leftrightarrows \equiv TiO^- . \quad (7)$$

Bridging hydroxyls are formed by a protonation of the oxygen bridges leading to a second cationic species $\equiv Ti\text{–}OH^+\text{–}Ti\equiv$:

$$\equiv Ti\text{–}OH^+\text{–}Ti\equiv - H^+ \leftrightarrows \equiv Ti\text{–}O\text{–}Ti\equiv \quad (8)$$

These reactions lead to the amphotheric properties of titanium surfaces. From the foregoing it can be concluded that the titanium dioxide surface displays a negative charge at physiological pH values. Although TiO_2 surfaces may also display chemisorptive properties [61], they are in general very stable and inert. One of the most important properties of a TiO_2 surface is the capability of forming hydroxyl groups, which may increase hydrophilicity. We could show that the boiling of a titanium surface in 5% HNO_3 leads to a reduction of the contact angle ($\theta_{Adv.}$) from 76° to 37° [2]. Probably the terminal hydroxyls are the ones to be modified by silane reagents such as aminopropyl triethoxy silane (APS) forming oxane bonds between the mineral surface and the silane as shown in **Fig. 4C**. Such modification reactions form the basis for functionalizing the titanium surface with biomolecules [2].

The use of titanium as a biomaterial goes back to papers in the 40ties and 50ties of the past century Bothe et al. [62] and Gottlieb and Levinthal [63]. In the 60ties Branemark introduced titanium into oral implantology and coined the word "osseointegraton" [64]. The

clinical long-term success of his dental implants was a landmark for titanium implantology as a whole [65].

Preparation of ultra-hydrophilic surfaces on transition metals

We have recently reported [2,5,6] that the surface of titanium, stainless steel (316L) and CoCrMo alloy can be enhanced by a novel wet-chemical method involving the treatment with chromosulfuric acid at 200-240 °C. The macroscopic appearance of such metals after acid treatment is shown in **Fig 5**. The previously electropolished surface loses its luster and becomes brown or gray. Fischer et al. [66] have shown that the acid treatment brings about a structured surface with a roughness Ra value between 0.88 and 1.13 µm. The surfaces for cp titanium and 316L stainless steel show a passive (oxide) layer with thicknesses between 10 and 50 nm [66]. Transmission electron microscopic diffraction patterns of 316L medicinal steel surfaces indicate a nano-crystalline microstructure with a fractal-like surface profile in the

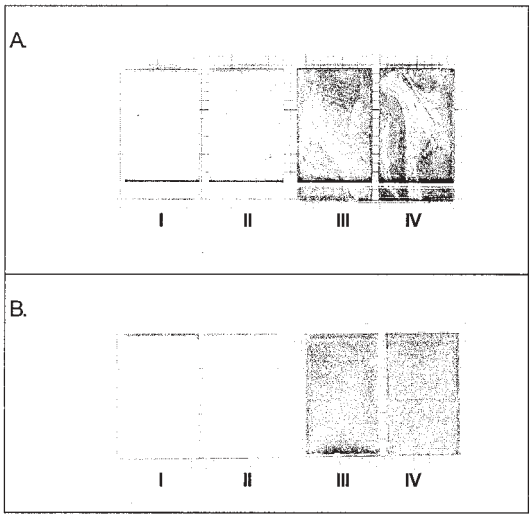

Fig. 5: Surface enhancement of titanium (A) and stainless steel (B) by chromosulfuric acid (CSA).

A. The titanium mini plates were heated to 240 °C for 60 minutes, I-II electropolished controls, III, IV CSA treatment. B. The electropolished stainless steel mini plates were heated to 230 °C for 60 min, I, II electropolished controls, III, IV CSA treatment. For further details see ref. [2] and Methods. From ref. [2].

nm-range [66]. Scanning electron micrographs of 316L steel and c.p. titanium mini plates are shown in **Fig. 6**. As can be seen the two metals show totally different surface topographies.

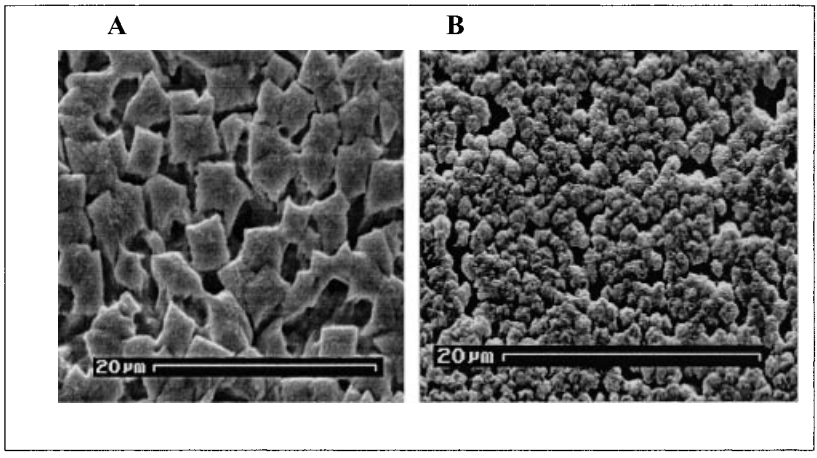

Fig. 6: Scanning electron microscopic images of surface enhanced i.e. chromosulfuric acid treated 316L stainless steel and cp titanium grade 2.
The scanning electron micrographs depict the surface of stainless steel (A) and titanium (B) after chromosulfuric acid treatment. For further details see legend to Fig. 5, Methods and the text.

The structures are due to the subtractive and additive action of chromosulfuric acid at temperatures > 200 °C. Apparently these surfaces display an uninterrupted transition into the bulk metal. Thus in Rockwell adhesion tests the indenter only leads to a plastic deformation of the surface without cracking or delamination [8].

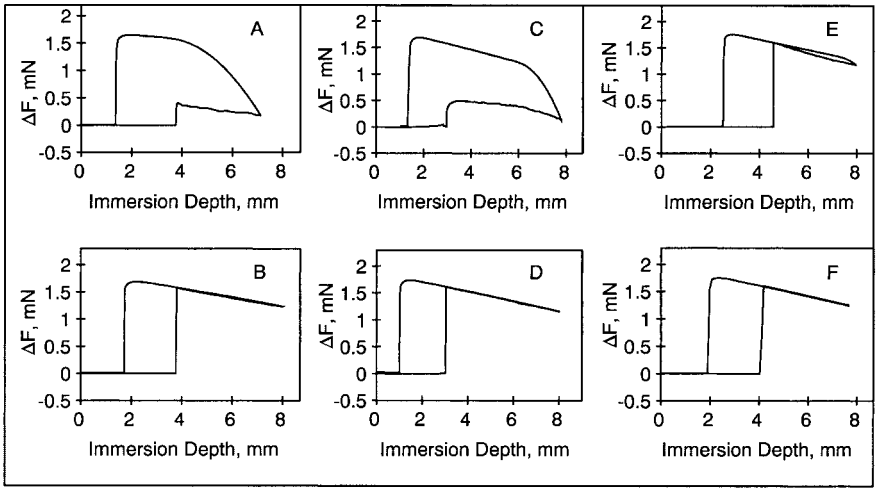

Fig. 7: Dynamic contact angle measurements of titanium (A,B), cobalt chromium alloy (C,D), 316 stainless steel (E) mini plates and highly polished quartz glass slide (F)
A. acetone cleaned electropolished titanium θ_A = 76°, θ_R = 18°; **B.** chromosulfuric acid treated electropolished titanium θ_A = 9°, θ_R = 9°; **C.** acetone cleaned electropolished CoCrMo alloy θ_A = 73°, θ_R = 7°; **D.** chromosulfuric acid treated electropolished CoCrMo alloy θ_A ~ 0°, θ_R ~ 0°; **E.** chromosulfuric acid treated 316 stainless steel θ_A = 4°, θ_R = ~0°; **F.** ultra-clean and ultra-smooth quartz glass θ_A ~ 0°, θ_R ~ 0°. Data from [2,4-6]. For further details see Methods, the text and [2,4-6].

Despite the very different surface topography both surfaces show identical wetting behavior. This is illustrated in **Fig. 7**, which shows dynamic contact angle profiles for cp titanium (**Fig. 7A, B**), CoCrMo alloy (**Fig. 7C, D**) and 316L steel (**Fig. 7E**) mini plates. Electropolished acetone cleaned metal surfaces generally display contact Angles of 70-80° (**Fig. 7A, C**) which according to the above definition are counted as mildly hydrophobic (see section 4.1.). Upon treatment with chromosulfuric acid the contact angles decrease to < 10° (**Fig. 7B, D, E**) with simultaneous disappearance of contact angle hysteresis, i.e. they become ultra-hydrophilic [6]. As a control an ultra clean and smooth (roughness: Ra ~ 2-3 nm) quartz glass plate is shown in **Fig. 7F** which is known to be extremely hydrophilic. As expected an advancing contact angle of ca. 0° and a contact angle hysteresis of ca. 0° (equality of advancing and receding contact angle) are measured. Thus chromosulfuric acid treated metal surfaces with a roughness of Ra = 1-2 μm display the properties of a perfectly homogenous

surface as ultra clean and ultra smooth quartz glass with a 300-500-fold lower roughness. Surfaces displaying dynamic contact angles < 10° with simultaneously absent contact angle hysteresis have been termed ultra-hydrophilic surfaces [6].

The disappearance of Contact angle hysteresis

Very characteristic of the CSA action on transition metals is the disappearance of contact angle hysteresis. As has been shown previously [2] the absence of hysteresis is not only due to the fact that the advancing contact angle approaches 0°. Already at an advancing contact angle of ~20° hysteresis disappears [2]. We conclude from our experiments that the disappearance of hysteresis is linked to the generation of a nano-scale homogeneity. This will be discussed below.

The question arises as to how we can explain the development of ultra-hydrophilicity. A severe restriction is that the Wenzel equation itself applies only to static contact angles [16,24]. If we suppose that the advancing dynamic contact angle corresponds to the static contact angle then some calculations can be made. Under this condition let us assume that the original contact angle (θ'_{GS}) on electropolished titanium before CSA-treatment was ca. 80° and the contact angle after CSA-treatment ($\cos \theta_{AS}$) was 0°, then $r = \cos 0° / \cos 80° = 5.8$ indicating that the surface area (solid-liquid interfacial area) should have increased by a factor of 5.8. It can be calculated that the Wenzel equation fails, if $r > 5.8$, since then $\cos \theta_{AS}$ will become grater than +1 (see eq. 3). The surface area increase measured for electropolished surfaces by confocal laser microscopy after the CSA treatment is however negligible (D. Lattner and H.P. Jennissen, unpublished) and can thus not explain the above phenomenon. Even on TPS-titanium alloy surfaces (see methods) with a roughness factor of $r \sim 20$ advancing contact angles of 30° can be measured (M. Chatzinikolaidou and H.P. Jennissen, unpublished). However on treatment with CSA the contact angle drops to 0° (see ref. [9]) without a change in surface roughness. Thus the Wenzel equation cannot explain these low contact angles.

As stated above the dynamic contact angles especially on rough surfaces are accompanied by metastable states. Since these were not considered by Wenzel, his equation is not stringently applicable to advancing and receding contact angles. These metastable states

are however considered in the papers by Johnson and Dettre [24,32]. Employing their model a fully different behavior for dynamic contact angles is found (see **Table 3**). For the case

Table 3: Dependence of static and dynamic contact angles on the roughness ratio of Wenzel as reported by Johnson and Dettre, 1964 for an initial contact angle $\theta = 45°$ at r = 1.0.

r	Wenzel $\theta_W°$	Johnson & Dettre (advancing) $\theta_A°$	Johnson & Dettre (receding) $\theta_R°$	Hysteresis $\Delta\theta_{AR}°$
1.00	45.0	45.0	45.0	0
1.05	40.7	59.6	31.4	28.2
1.10	37.7	64.9	22.1	42.8
1.15	34.4	69.2	15.0	54.2
1.20	30.9	72.5	9.1	63.4
1.25	27.5	74.8	4.3	70.5
1.30	23.3	77.0	~0	77.0
1.35	18.7	78.9		
1.40	12.7	80.2		
1.45	~0	81.5		

$\theta_W°$: Most probable contact angles calculated by Johnson & Dettre [24] from the Wenzel Equation (eq. 3)
$\theta_A°$: Possible advancing angles calculated according to the Model of Johnson & Dettre
$\theta_R°$: Possible receding angles calculated according to the Model of Johnson & Dettre
$\Delta\theta_{AR}°$: Contact angle hysteresis ($\Delta\theta_{AR}° = \theta_A° - \theta_R°$)
The values of Table 3 were obtained from the paper of Johnson and Dettre, 1964 [24] by digitizing the curves in Fig. 11 of that paper.

$\theta < 90°$ the advancing contact angle increases and the receding contact angle decreases as a function of surface roughness leading to an overall increase in contact angle hysteresis **Table 3**. The case for $\theta > 90°$ is even more complex [24] and will not be treated further here. Thus we come to the basic conclusion that for surfaces with $\theta < 90°$ an increase in roughness factor should lead to an increase in contact angle hysteresis. This conclusion is of importance for the present work since we have the paradox situation that in the case of ultra-hydrophilic surfaces the classical Wenzel equation [21] predicts a several fold increase in roughness factor from the decrease in contact angle while the model of Johnson and Dettre [24,32] predicts a decrease in roughness factor from the disappearance of contact angle hysteresis. In reality the roughness factor remains practically constant on treatment of the metal with chromosulfuric acid. Thus it is quite possible that ultra-hydrophilicity in the absence of hysteresis on microscopically rough surfaces of Ra = 1-40 μm (i.e. inverse Lotus effect) found after chromosulfuric acid

treatment of metals at high temperatures must be explained on the basis of novel chemical and possibly ultrastructural properties. The generation of new hydroxyl and/or ionic groups on the surface as well as the formation of a novel nano-structure [66] may be the cause. Considering the intrinsic contact angle approach of Marmur [30] one definite statement can be made: "as the Young contact angle approaches zero the difference to the intrinsic contact angle also approaches zero, so that at a contact angle of zero the Young equation is valid".

The inverse Lotus Effect

We have defined ultra-hydrophilicity as the co-existence of dynamic contact angles < 10° with absent contact angle hysteresis on microscopically rough surfaces [6]. It was suggested that these properties cannot be attributed to a smoothness and homogeneity resulting from polishing, but moreover to novel physicochemical structures and/or functional chemical groups. Thus in contradistinction to the Lotus effect for ultra-hydrophobicity we have called the presence of ultra-hydrophilicity on a microscopically rough surface Inverse Lotus Effect. The extreme hydrophilicity and absence of hysteresis on a microscopically rough metal surface forms a paradox which remains to be elucidated. It is suggested that ultra-hydrophilic ($\theta_A \cong \theta_R < 10°$) and ultra hydrophobic ($\theta_A \cong \theta_R > 130°$) surfaces comprise a new group of ultraphilic surfaces ("extremes loving").

Histophilicity and Bioactivity

The question could be asked, how chromosulfuric acid structured metal surfaces can be of use in medicine. Since novel metallic biomaterials today only rarely involve changes in the bulk metal but moreover are primarily determined by novel surfaces, we believe that they may be termed a novel form of metallic biomaterial due to the displayed Inverse Lotus effect. According to the critical surface tension model of Baier ultra-hydrophilic surfaces should be strongly histophilic i.e. bioadhesive. Ultraphilic surfaces may therefore form the basis of a new generation of advanced metallic and possibly non-metallic biomaterials for human applications. Such materials can be used directly as bone implants because of their ultra-hydrophilic and osteophilic properties. Such hydrophilic surfaces can also be expected to increase bioadhesion of other tissues in the sense of general histophilicity. From preliminary experiments (to be published) it can be expected that the bone-implant-contact will increase from 30-40% to maybe > 50% which would lead to an earlier implant-bone force conductance

and may allow an earlier functional implant loading and usage. Such surfaces have already been employed with good success in vivo [5,9,10].

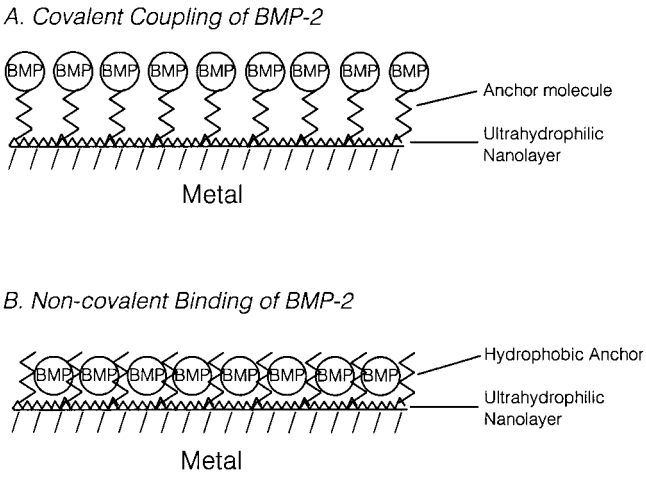

Fig. 8: Scheme of the immobilization of rhBMP2 on ultra hydrophilic implant materials

The Immobilized amount of BMP-2 on a titanium surface (r = 1.3-20) can vary from 0.15 to 8 μg/cm^2. For further details see ref. [2,4,5,8,10] and the text.

Alternatively we have also suggested that the ultra-hydrophilic surface be employed as the priming coat for subsequent functionalization reactions aimed at synthesizing a biologically active surfaces with signaling molecules (i.e. biocoat) either for in vitro or in vivo tissue engineering or biomimetics [67]. The priming coat is intended to constitute the long-term tissue implant interface (decades), whereas the biocoat is only designed for a short-term tissue-implant interface (months maybe 1 or 2 years at the most) bearing molecular recognition properties. After degradation of the biocoat the priming coat takes over for the rest of the implant lifetime. We have constructed such a biologically active biocoat by immobilizing rhBMP-2 covalently and non-covalently directly on the titanium surface [2,4,5,8,10]. This is shown schematically in **Fig. 8**. Proteins can be immobilized in two principle ways: covalently and non-covalently. After the silanization step (**Fig. 4C**) proteins may be coupled by carbonyl diimidazole to the ε-amino group of lysine residues on retains a

biologically active species capable of eliciting alkaline phosphatase induction in the osteoblast cell line MC3T3-E1 as shown in **Fig. 9**. The MC3T3-E1 cells are seeded on the covalently

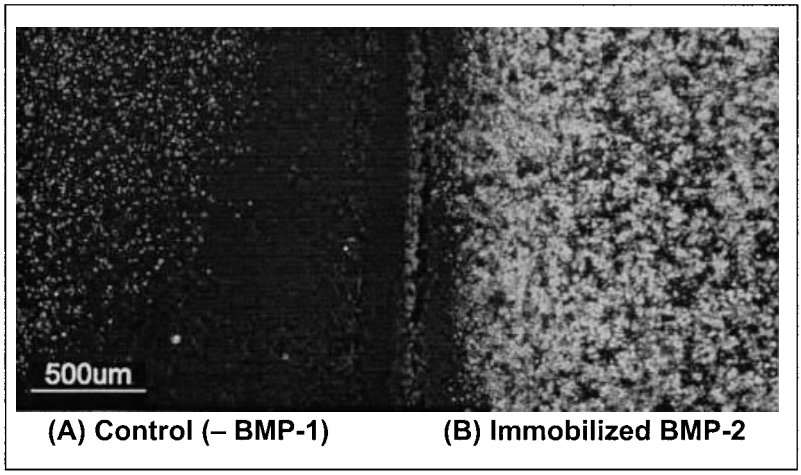

Fig. 9: In vitro bioassay of rhBMP-2 immobilized on CSA treated titanium miniplate surface . MC3T3-E1 cells were seeded on sterile titanium mini plates which had either been sham modified (A) (= controls) or coated with rhBMP-2 ~ 1.6 µg/cm^2 by covalent immobilization (B) and placed in the wells of a 48 well microtiter plate for 6 days. After fixation with paraformaldehyde alkaline phosphatase activity was determined with ELF-97 (bright fluorescence) in a fluorescence microscope. From ref. [8]. For further details see Methods, text and ref. [8].

immobilized rhBMP-2 on the metal surface and allowed to grow to confluence for 6 days. As can be seen in **Fig. 9** practically no alkaline phosphatase is induced on the control mini plate, although it contains an identical number of cells as measured by nuclear stain (not shown). In contrast there is a very strong induction of alkaline phosphatase in those cells which are in contact with either non-covalently (i.e. released) or covalently immobilized rhBMP-2 (= intense green color). Thus rhBMP-2 has retained its biological activity after the immobilization procedure [8].

Conclusions

From the data it can be concluded that a novel ultra-hydrophilic surface is created on titanium and stainless steel (316L) by the chromosulfuric acid (CSA) method which cannot be explained by an analogy to ultra-clean and ultra-smooth quartz glass. Indications are that a novel structuring of the surface on a micro- and nanometer scale may be responsible for these properties in a way comparable to the microstructures of ultra-hydrophobic surfaces (Lotus-effect) only of the opposite nature. Alternatively specific chemical reactions may modify the surface in a novel way as too display ultra-hydrophilicity. The novel surface structures also enhance the capacity for the coupling proteins to the surface. CSA-treated titanium implants are biocompatible and in connection with rhBMP-2 dramatically increase bone growth.

Acknowledgments

This work was supported by the Ministerium für Schule, Wissenschaft und Forschung NRW (IV A 6 – 214 005 97). Ref. [68] is also acknowledged.

[1] McMillin, C. *Biomaterial Forum* **1999,** *21,* 5.
[2] Jennissen, H. P.; Zumbrink, T.; Chatzinikolaidou, M.; Steppuhn, J. *Materialwiss. Werkstofftech.* **1999,** *30,* 838-845.
[3] Jennissen, H. P. *PCT Patent WO9926674A2 (Priority date Nov. 24, 1997)* **1999,** pp. 1-29 (+ 5 Figs), Munich.
[4] Chatzinikolaidou, M.; Laub, M.; Rumpf, H. M.; Jennissen, H. P. *Materialwiss. Werkstofftech.* **2002,** *33,* 720-727.
[5] Jennissen, H. P.; Chatzinikolaidou, M.; Rumpf, H. M.; Lichtinger, T.; Müller, R. *DVM Bericht* **2000,** *313,* 127-140.
[6] Jennissen, H. P. *Biomaterialien* **2001,** *2,* 45-53.
[7] Wang, R.; Hashinmoto, K.; Fujishima, A.; Kitamura, A.; Shimohigoshi, M.; Watanabe, T. *Nature* **1997,** *388,* 432.
[8] Chatzinikolaidou, M.; Zumbrink, T.; Jennissen, H. P. *Materialwiss. Werkstofftech.* **2003,** *34,* 1106-1112.
[9] Lichtinger, T. K.; Müller, R. T.; Schürmann, N.; Wiemann, M.; Chatzinikoleidou, M.; Rumpf, H. M.; Jennissen, H. P. *Materialwiss. Werkstofftech.* **2001,** *32,* 937-941.
[10] Voggenreiter, G.; Hartl, K.; Chatzinikolaidou, M.; Rumpf, H. M.; Jennissen, H. P. *Materialwiss. Werkstofftech.* **2001,** *32,* 942-948.
[11] Adamson, A. W. Physical Chemistry of Surfaces; John Wiley & Sons: New York, 1990; pp 389-402.
[12] Jennissen, H. P.; Zumbrink, T.; Chatzinikolaidou, M.; Steppuhn, J. *Materialwiss. Werkstofftech.* **1999,** *30,* 838-845.
[13] Wiemann, M.; Rumpf, H. M.; Bingmann, D.; Jennissen, H. P. *Materialwiss. Werkstofftech.* **2001,** *32,* 931-936.
[14] Young, T. *Philos. Trans. Roy. Soc. London* **1905,** *95,* 65-87.

[15] Andrade, J. D.; Smith, L. M.; Gregonis, D. E. The Contact Angle and Interface Energetics. In *Surface and Interfacial Aspects of Biomedical Polymers*; Andrade, J. D., Ed.; Plenum Press: New York, London, 1985; Chapter 1, Surface Chemistry and Physics.
[16] Asthana R.; Sobczak, N. *JOM-e (Journal of Metals, electronic supplement)* **2000,** *52,* 1-15.
[17] Chattoraj, D. K.; Birdi, K. S. Adsorption and the Gibbs Surface Excess; Plenum Press, New York & London: 1984; pp 250.
[18] Hunter, R. J. Foundation of Colloid Science; Clarendon Press: oxford, 1993; pp 290-315.
[19] LaPorte, R. J. Hydrophilic Polymer Coatings for Medical Devices; Technomic Publishing Co., Inc.: Lancaster PA, USA, 1997; pp 3-17.
[20] Wenzel, R. N. *J. Phys. & Colloid. Chem.* **1949,** *53,* 1466-1467.
[21] Wenzel, R. N. *Ind. Eng. Chem. (Industrial Edition)* **1936,** *28,* 988-994.
[22] Zisman, W. A. *Adv. Chem. Ser.* **1964,** *43,* 1-51.
[23] Jennissen, H. P. *in "Surface and Interfacial Aspects of Biomedical Polymers" Vol. 2, Protein Adsorption* **1985,** *2,* 295-320.
[24] Johnson, R. E.; Dettre, R. H. *Adv. Chem. Ser.* **1964,** *43,* 112-135.
[25] Jennissen, H. P. *Phys Fluids* **2005,** *17,* in print.
[26] Barthlott, W.; Neinhuis, C. *Planta* **1997,** *202,* 1-8.
[27] Huh, C.; Mason, S. G. *J. Colloid Interface Sci.* **1977,** *60,* 11-38.
[28] Cassie, A. B. D. *Discuss. Faraday Soc.* **1948,** *3,* 11-16.
[29] Crawford, R.; Koopal, L. K.; Ralston, J. *Colloids and Surfaces* **1987,** *27,* 57-64.
[30] Marmur, A. *J. Adhesion Sci. Technol.* **1992,** *6,* 689-701.
[31] Swain, P. S.; Lipowsky, R. *Condensed Matter (www-admin@arxiv. org)* **1998,** *9809089,* 1-10.
[32] Dettre, R. H.; Johnson, R. E. *Adv. Chem. Ser.* **1964,** *43,* 136-144.
[33] Heimann, R. B. Plasma Spray Coating: Principles and Applications; VCR: Weinheim, 1996; pp 155-159.
[34] Jennissen, H. P. *Int. J. Bio-Chromatography* **2000,** *5,* 131-163.
[35] Israelachvili, J. N. Intermolecular and Surface Forces; Academic Press: London, New York, 1985; pp 105, 207.
[36] Ben Naim, A.; Wilf, J.; Yaacobi, M. *J. Phys. Chem.* **1973,** *77,* 95-102.
[37] Jennissen, H. P. *Hoppe-Seyler's Z. Physiol. Chem.* **1976,** 1727-1733.
[38] Van Damme, H. Protein Adsorption at the Solid-Liquid Interface; Thesis, Uniersity of Twente, NL, CIP-Data Koninklijke Bibliothek: Den Haag, 1990; pp 11.
[39] Sacher, E. The Determination of Surface Tensions of Solid Films. In *Surface Characterization of Biomaterials*; Ratner, B. D., Ed.; Elsevier Science Publishers B.V.: Amsterdam, 1988.
[40] Baier, R. E. *Bull N Y Acad Med* **1972,** *48,* 257-272.
[41] Thomas, K. A. *Orthopedics* **1994,** *17,* 267-278.
[42] Schakenraad, J. M.; Busscher, H. J.; Wildevuur, C. R. H.; Arends, J. *J. Biomed. Mater. Res.* **1986,** *20,* 773-784.
[43] van Kooten TG; Schakenraad JM; van der Mei HC; Busscher HJ *Biomaterials* **1992,** *13,* 897-904.
[44] Pringle JH; Fletcher M *Appl Environ Microbiol* **1986,** *51,* 1321-1325.
[45] Jones, M. I.; McColl, I. R.; Grant, D. M.; Parker, K. G.; Parker, T. L. *J. Biomed. Mater. Res.* **2000,** *52,* 413-421.
[46] Takebe, J.; Itoh, S.; Okada, J.; Ishibashi, K. *J. Biomed. Mater. Res.* **2000,** *51,* 398-407.
[47] Becker, J.; Meissner, T.; Neukam, F. W.; Graf, H. L.; Reichart, P. *Z. Zahnärztl. Implantol.* **1991,** *7,* 162-169.
[48] Freundlich, H. Kapillarchemie; Akademische Verlagsgesellschaft M.B.H.: Leipzig, 1923; pp 211-219.
[49] Wolf, R. M. H. O. E. L. J. *Acta Dermatovenerol Croat.* **2001,** *11,* 158-162.
[50] Schlosser, E. Fast Food Nation; Houghton-Mifflin: Boston, 2001; pp 111-132.
[51] Incledon C; Paquet C; Johnston A; Jairam R; Lam H. *J Pharm Biomed Anal* **2003,** *31,* 413-420.
[52] Rowe RC *J Pharm Pharmacol* **1984,** *36,* 596-572.
[53] Anderson, R. R. *Arch. Dermatol.* **2001,** *137,* 210-212.
[54] Edel, J.; Marafante, E.; Sabbioni, E. *Hum. Toxicol.* **1985,** *4,* 177-185.
[55] Thomas, P.; Barnstorf, S.; Summer, B. *Biomaterialien* **2001,** *2,* 35-44.
[56] McCue, J. P. Biological Effects of Titanium; Alan Lucas & Associate: East Greenwich, RI 02818, USA, 2003; pp 22-32.
[57] Larson, I.; Attard, P. *J. Colloid Interface Sci.* **2000,** *227,* 152-163.
[58] Li, J. *Biomaterials* **1993,** *14,* 229-232.
[59] Feiler, A.; Larson, I.; Jenkins, P.; Attard, P. *Langmuir* **2000,** *16,* 10269-10277.

[60] Cacciafesta, P.; Humphris, A. D. L.; Jandt, K. D.; Miles, M. J. *Langmuir* **2000,** *16,* 8167-8175.
[61] Robert, D.; Parra, S.; Pulgarin, C.; Krzton, A.; Weber, J. V. *Appl. Surf. Sci.* **2000,** *167,* 51-58.
[62] Bothe, R. T.; Beaton, L. E.; Davenport, H. A. *Surg. Gynaecol. Obstet.* **1940,** *71,* 598-602.
[63] Gottlieb, S.; Leventhal, M. D. *J. Bone and Joint Surg.* **1951,** *33-A,* 473-474.
[64] Branemark, P. I.; Adell, R.; Breine, U.; Hansson, B. O.; Lindstrom, J.; Ohlsson, A. *Scand. J. Plast. Reconstr. Surg.* **1969,** *3,* 81-100.
[65] Branemark, P. I.; Hansson, B. O.; Adell, R.; Breine, U.; Lindstrom, J.; Hallen, O.; Ohman, A. *Scand. J. Plast. Reconstr. Surg. Suppl* **1977,** *16,* 1-132.
[66] Fischer, A.; Jennissen, H. P.; Chatzinikolaidou, M.; Wiemann, M.; Bingmann, D.; Büscher, R.; Sawitowski, T. *Abstract Communication in "Proceedings Materials Week 2000 25-28 Sept. 2000, Munich, Germany; Online URL: http://www. materialsweek. org* **2000.**
[67] Jennissen, H. P. *Annals N. Y. Acad. Sci.* **2002,** *961,* 139-142.
[68] Schiermeier, Q.; Weydt, P. *Nature* **2000,** *404,* 217.